

Analysis of DSN PPM Support During Voyager 2 Saturn Encounter

C. D. Bartok
Control Center Operations

The Precision Power Monitor (PPM) is a precision radiometric instrument used to improve the efficiency of signal reception by the Deep Space Network. Real-time estimates of the system operating temperature, the present (signal + noise)-to-noise ratio, and the signal power are utilized to increase the accuracy and resolution of the received spacecraft signal.

Due to the critical nature of Radio Science data returning from Voyager 2 at Saturn Encounter, PPM support was required. The task was undertaken to validate the performance of equipment technically under research and development in time to meet the encounter deadline. Initial studies revealed PPM performance to be out of tolerance. Action was immediately taken to identify the system problems. Using data analysis as feedback, the system failures were identified and corrected in time to contribute to the encounter support efforts. As a result, the Radio Science data were collected successfully.

I. Background

The Precision Power Monitor, or PPM, functions as a precision radiometric instrument for the Receiver-Exciter Subsystem. The PPM is used to furnish real-time estimates of the system operating temperature (T_{op}), the present (signal + noise)-to-noise ratio $(S + N)/N$, and the signal power S of the received spacecraft signal. The main components comprising the PPM are the S-band and X-band noise diode assemblies, the noise-adding radiometer (NAR), and the Precision Signal Power Monitor (PSPM).

The Deep Space Network (DSN) mode of operation is the primary application function of the PPM. The PPM uses the

intermediate frequency (IF) output from either the Block III or Block IV System Receivers as input (see Figs. 1 and 2). From this input the noise temperature is obtained by using NAR techniques. These are designed such that the noise added by the NAR does not degrade T_{op} by more than 0.1 dB.

From the same input the PSPM utilizes a fast Fourier transform (FFT) algorithm to measure the spectrum of the spacecraft signal. This spectrum is operated upon to form the (signal + noise)-to-noise ratio. Knowledge of this ratio and the noise temperature is used to calculate the noise power. From these data the signal power S is measured. The resultant PPM output provides continuously updated display and communication of T_{op} , $(S + N)/N$, and S to the station.

II. S-Band and X-Band Noise Diode Assemblies

The S-band and X-band noise diode oven assembly and power supply assembly provide a modulated stable noise signal at any one of seven preset levels. The noise is injected into the low-noise input coupler through the calibration assembly for the respective traveling wave maser (TWM), as shown in Figs. 1 and 3. The composite signal is extracted from the DSN receiver at IF and processed by the PPM to provide real-time system temperatures and signal level measurements.

The seven diode levels are calibrated against a precision ambient termination using a Y-factor method with the antenna looking at the cold sky in the zenith position and the maser input switching from the antenna to the ambient load (see Fig. 3). After calibration, the diode noise levels are used to provide reference values for NAR and PSPM processing.

III. NAR Subassembly

The NAR function measures the S-band or X-band operating temperature T_{op} of a Deep Space Station (DSS). The temperature can be measured over a range of 10 to 400 K with a specified accuracy of 0.3 K and signal resolution of 0.1 dB_m.

The fundamental equation describing the operation of the NAR is:

$$T_{op} = \frac{T_N}{(Y - 1)}$$

where

T_{op} = system operating noise temperature, kelvin
(defined at system input reference plane)

T_N = noise diode injected noise temperature, kelvin
(defined at system input reference plane)

Y = Y-factor = $(V_2 + \alpha V_2^2)/(V_1 + \alpha V_1^2)$

V_2 = square law detector output voltage, diode on,
volts

V_1 = square law detector output voltage, diode off,
volts

α = detector nonlinearity constant, volts⁻¹ (= 0 in an ideal detector)

The NAR noise temperature measurement resolution is given by:

$$\Delta T = 2T_{op}(1 + T_{op}/T_N)(B\tau)^{1/2}$$

where

B = predetection bandwidth, hertz

τ = integration time, seconds

The PPM software provides for automatic operation of the NAR. The NAR channel receives the "counts" from the voltage-to-frequency converter that are proportional to the product of the system operating temperature and the system gain (see Fig. 3). An assumption of $T_{op} = 40$ K is initially made which caused the NAR to select the $T_N = 0.50$ K noise diode and to integrate for 56 seconds. Once the measured value is available, the NAR makes a decision on which of the seven preset noise diodes to use and how long to integrate (see Fig. 4). This reiteration allows the noise temperature measurement accuracy and resolution to be 0.1 dB and offers the data in the minimum possible time.

Concurrently, the NAR monitors the output to insure that it is within the expected temperature range. The output, T_{op} , becomes an operator display which updates automatically as frequently as the existing noise temperatures change.

IV. PSPM Subassembly

The PSPM provides knowledge of received spacecraft signal power. By observing changes in power level from predicted performance, spacecraft anomalies can be diagnosed and examined. In addition, as each DSN station is brought into view of the spacecraft by the Earth's rotation, the measurement of received signal power serves to validate individual station performance by comparison of station-to-station readings.

The technique for power measurement consists first of measuring the power spectrum of the received signal in a bandwidth just wide enough to observe the background noise. A typical power spectrum is shown in Fig. 5. Suitable manipulation of the power spectrum utilizing a FFT algorithm yields the (signal + noise)-to-noise ratio:

$$R = (S + N)/N.$$

Since T_{op} is known, as is the NAR prediction bandwidth B , the noise power is calculated as

$$P_N = kT_{op}B$$

where k = Boltzman's constant. The signal power is then determined:

$$S = P_N(R - 1),$$

but substituting the expression for P_N yields

$$S = kT_{op}B(R - 1).$$

The PSPM function measures either the S-band or X-band carrier power over a system temperature operating range from 10 to 400 K, and a signal power range from -120 dB_m to -165 dB_m . The PSPM operates automatically by first assuming a signal power. After the first measurement of the signal, the known signal level is used to set the integration time for improved signal power measurement resolution ΔS (see Fig. 6). The measurement procedure is reiterated for maximum resolution and accuracy. The outputs $(S + N)/N$ and S are provided to the station as continuously updating displays.

V. PPM Performance

During the Voyager 2 Saturn Encounter the PPM supported Radio Science data collection. The PPM was considered to be under research and development prior to this encounter. However, since the critical nature of the Radio Science data returning from Voyager 2 required PPM support, the task was undertaken to validate the performance of the PPM in time to meet the encounter deadline.

Although the three 64-meter-diameter antenna sites of the DSN were equipped with PPM hardware, only the NAR sub-assembly was utilized for support procedures. An intensive effort was launched to develop a method of analyzing the operating temperature of the antenna system. Each 64-meter station tracking Voyager 2 for 10- to 12-hour periods recorded

NAR temperature data points every five seconds throughout those periods. The resultant data files were plotted so that the operating temperature could be visualized as a function of time.

A tracking pass corresponds to the time span as the spacecraft comes into view near the horizon and continues as it crosses the local sky until it travels out of view near the horizon. Thus, the data plots inherently illustrate operating temperature as a function of elevation as well as a function of time. Comparing the curvature of the data plots with nominal system noise temperature versus elevation test plots further confirms this relationship (see Figs. 7, 8 and 9). These test plots indicate acceptable PPM system temperatures under ideal test conditions for each 64-meter station operating at X-band frequencies. Nominal system temperatures at S-band operation average about three degrees less.

The actual data plots (Figs. 10-12) showed interesting results. The initial data plots for each of the stations revealed PPM performance out of tolerance. Encounter support was not possible with the evident PPM problems. Action was immediately taken to locate the source of the system problems. Using the data plots as feedback, the system failures were identified, located and corrected one by one. Analysis continued up until encounter to monitor the condition of the PPM performance. As the plots depict, the PPM was brought up to acceptable standards and validated in time to contribute to encounter support. PPM plots at all three 64-meter DSS sites showed system noise temperature within performance specifications and relatively unperturbed during encounter. Radio Science data collection was successful.

Acknowledgment

A special thanks is due Dorin M. Lasco for developing software enabling the manipulation and reduction of vast quantities of data into manageable files.

Bibliography

Winkelstein, R., "Precision Signal Power Measurement," *JPL Quarterly Technical Review*, Volume 2, Number 2, July 1972, pp. 18-24.

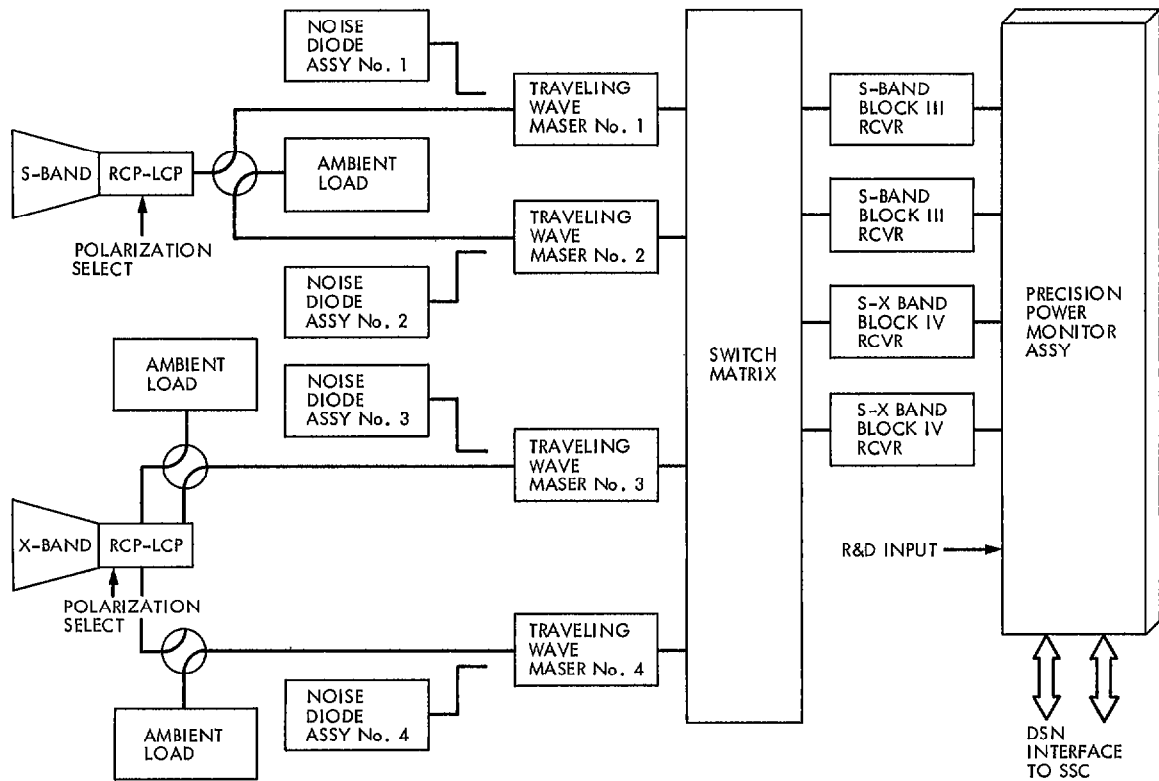


Fig. 1. System block diagram

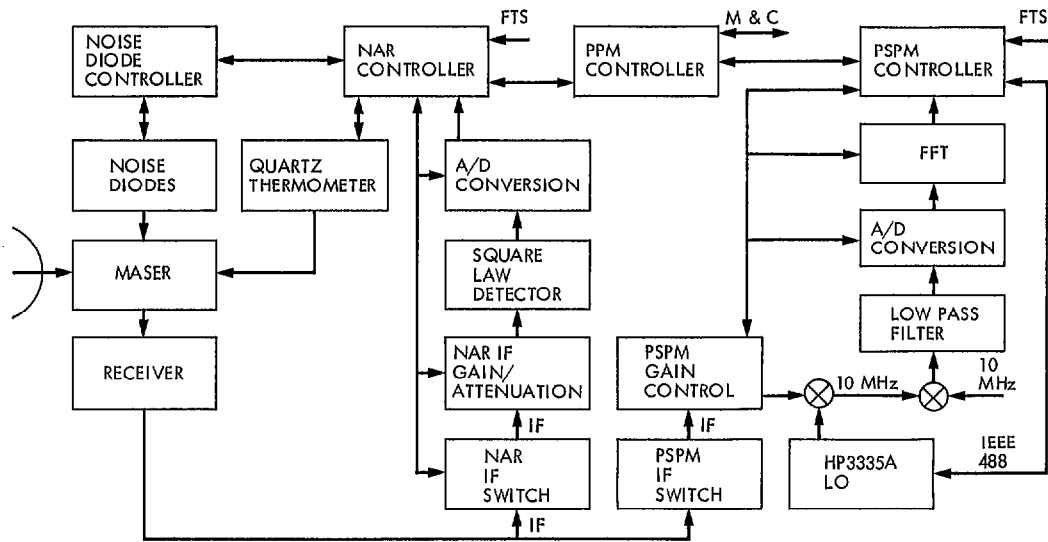


Fig. 2. PPM functional block diagram

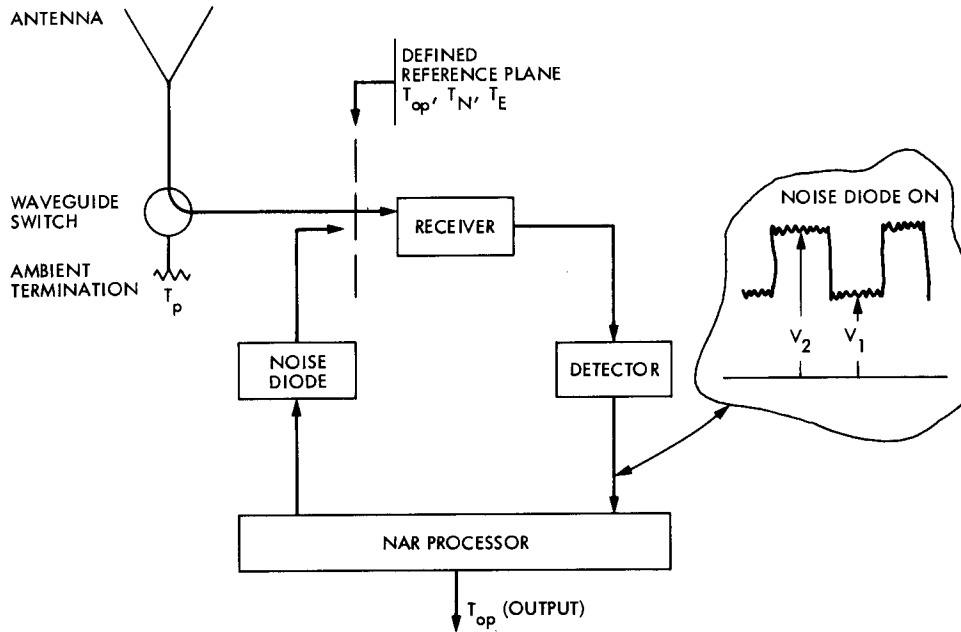


Fig. 3. Microwave receiving system showing NAR configuration

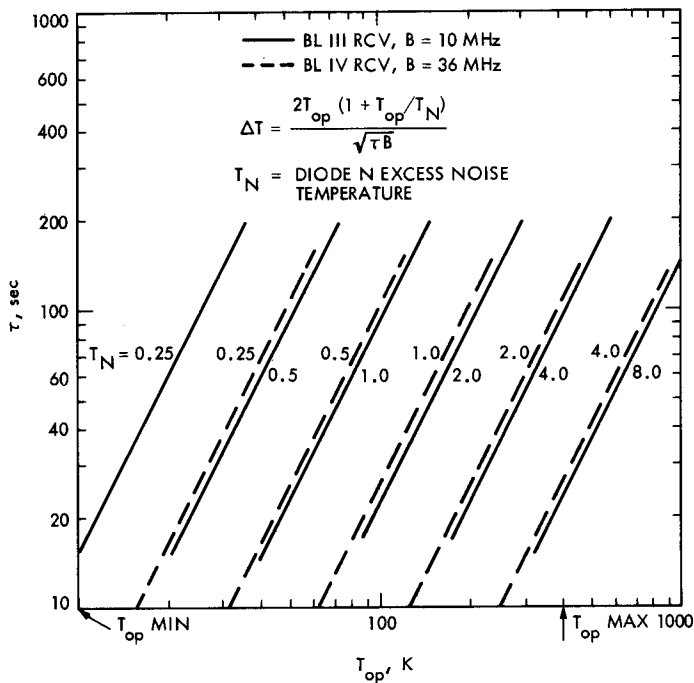


Fig. 4. Integration time τ required for 2% accuracy versus T_{op} as a function of IF bandwidth

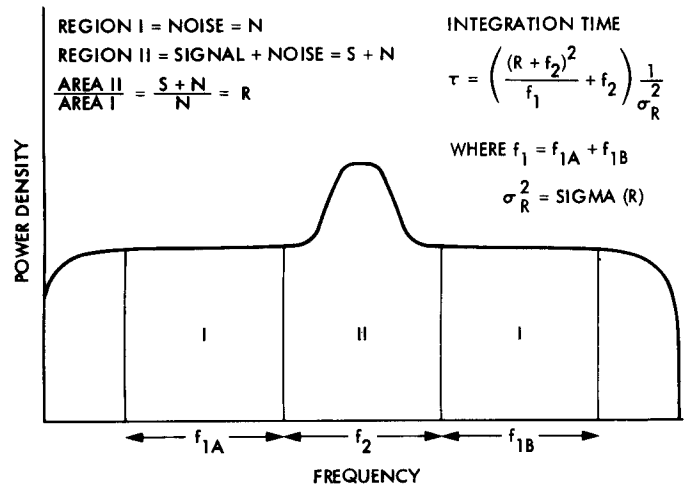


Fig. 5. Precision signal power measurement

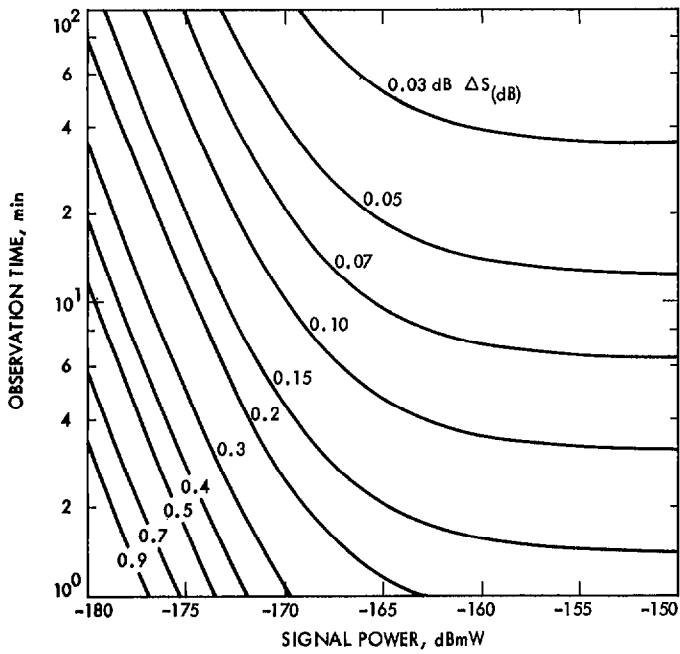


Fig. 6. PSPM required observation time

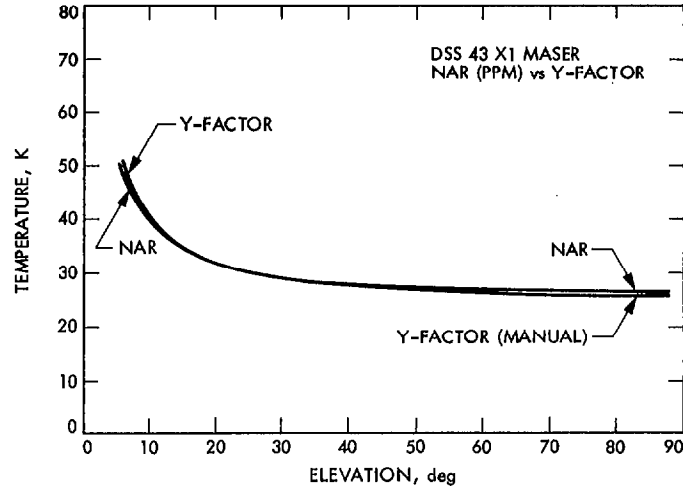


Fig. 8. System temperature versus antenna elevation, X-band, DSS 43

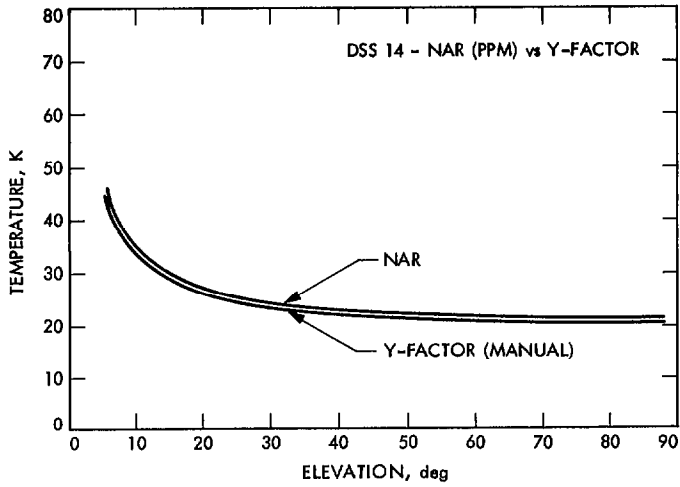


Fig. 7. System temperature versus antenna elevation, X-band, DSS 14

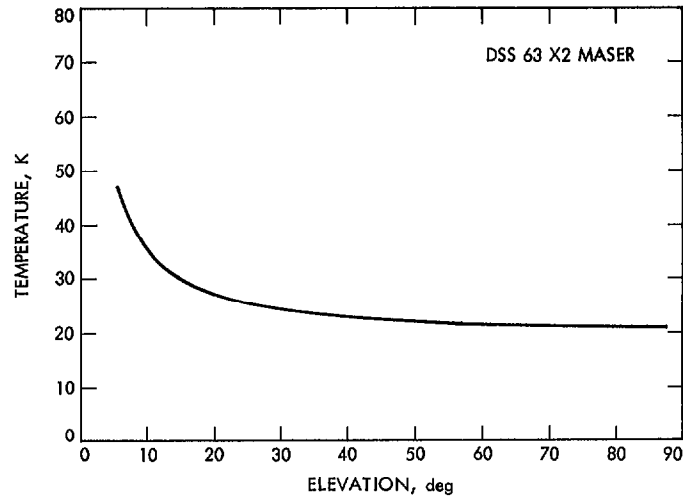


Fig. 9. System temperature versus antenna elevation, X-band, DSS 63

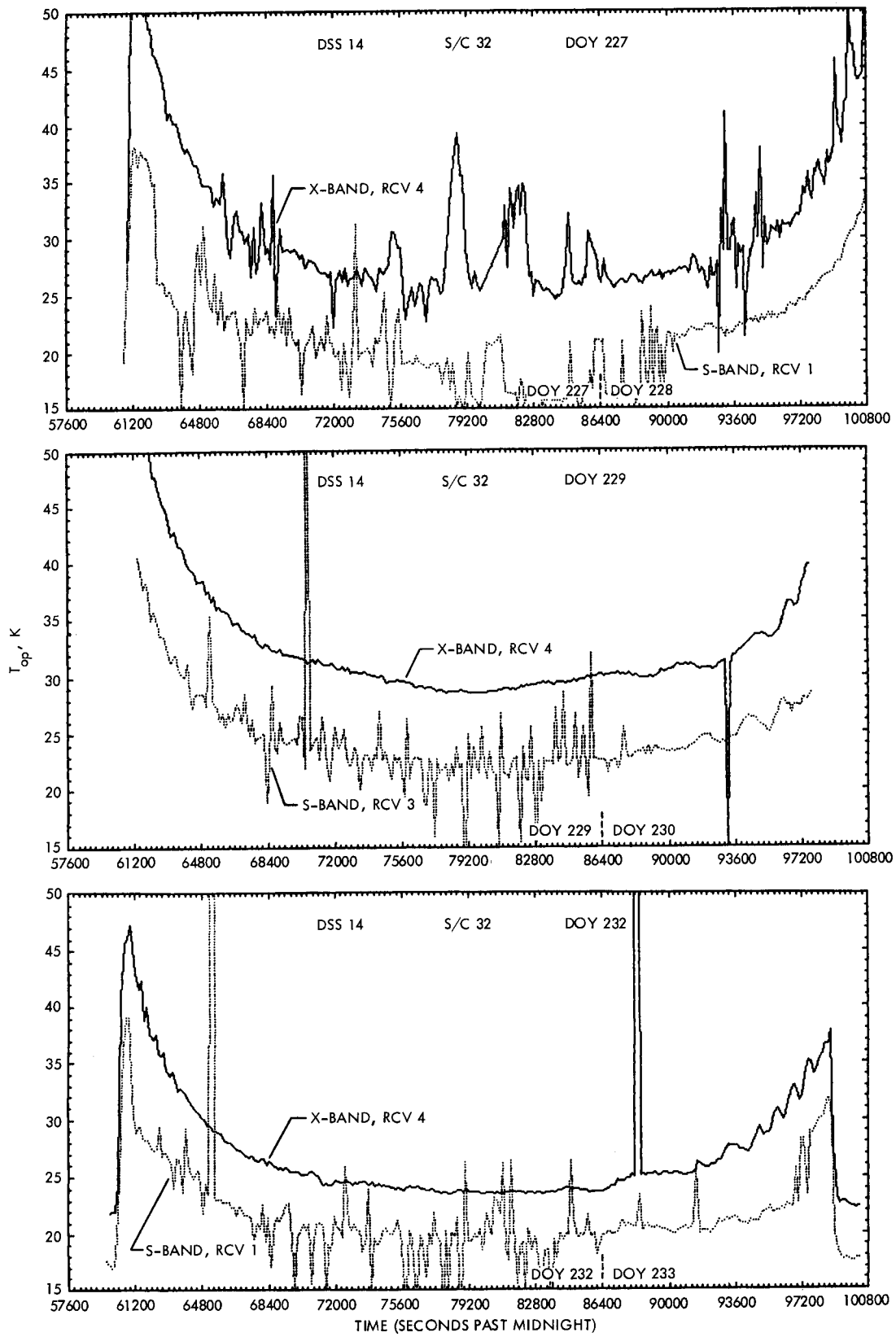


Fig. 10. System noise temperature plot—Goldstone, California

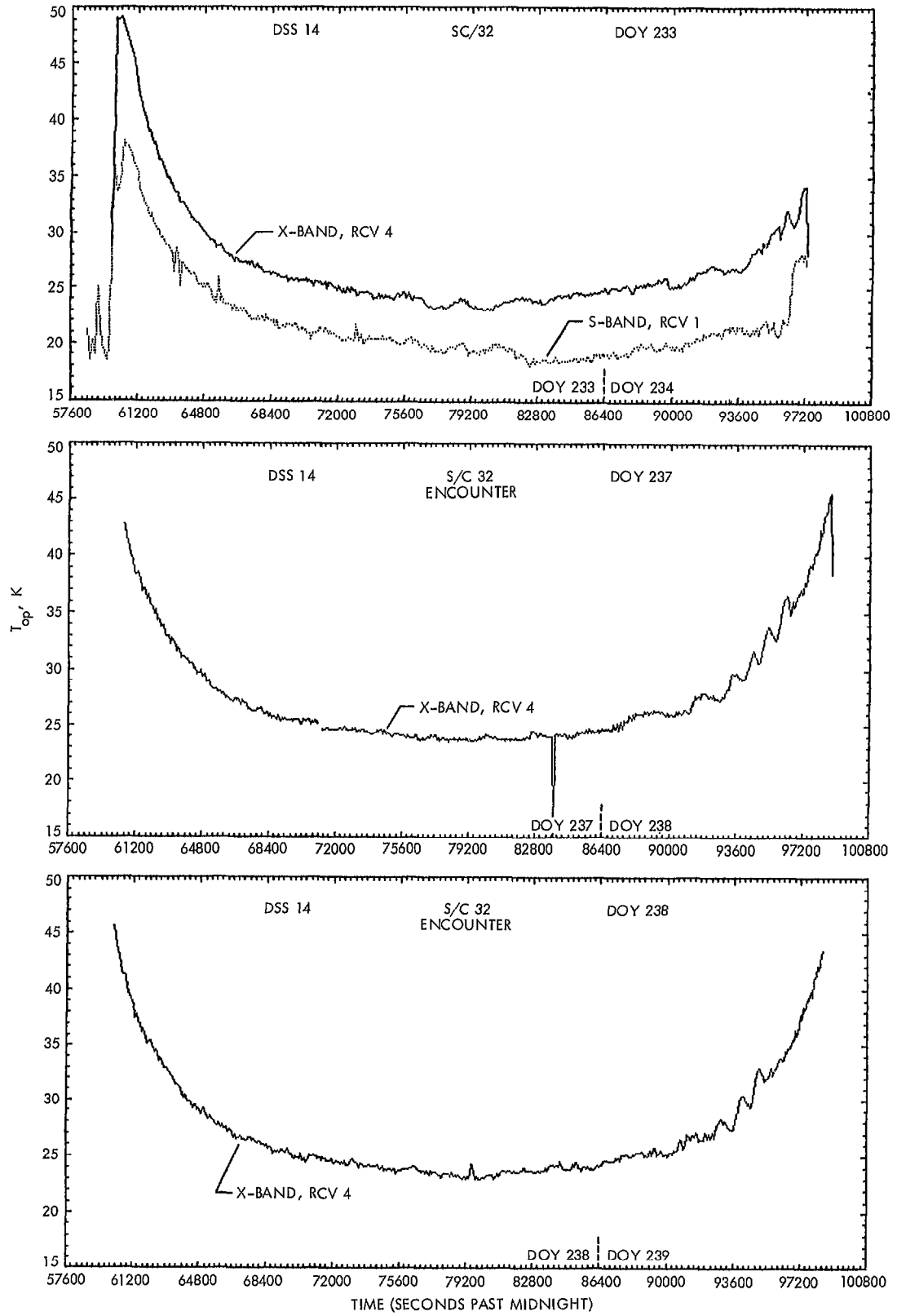


Fig. 10 (contd)

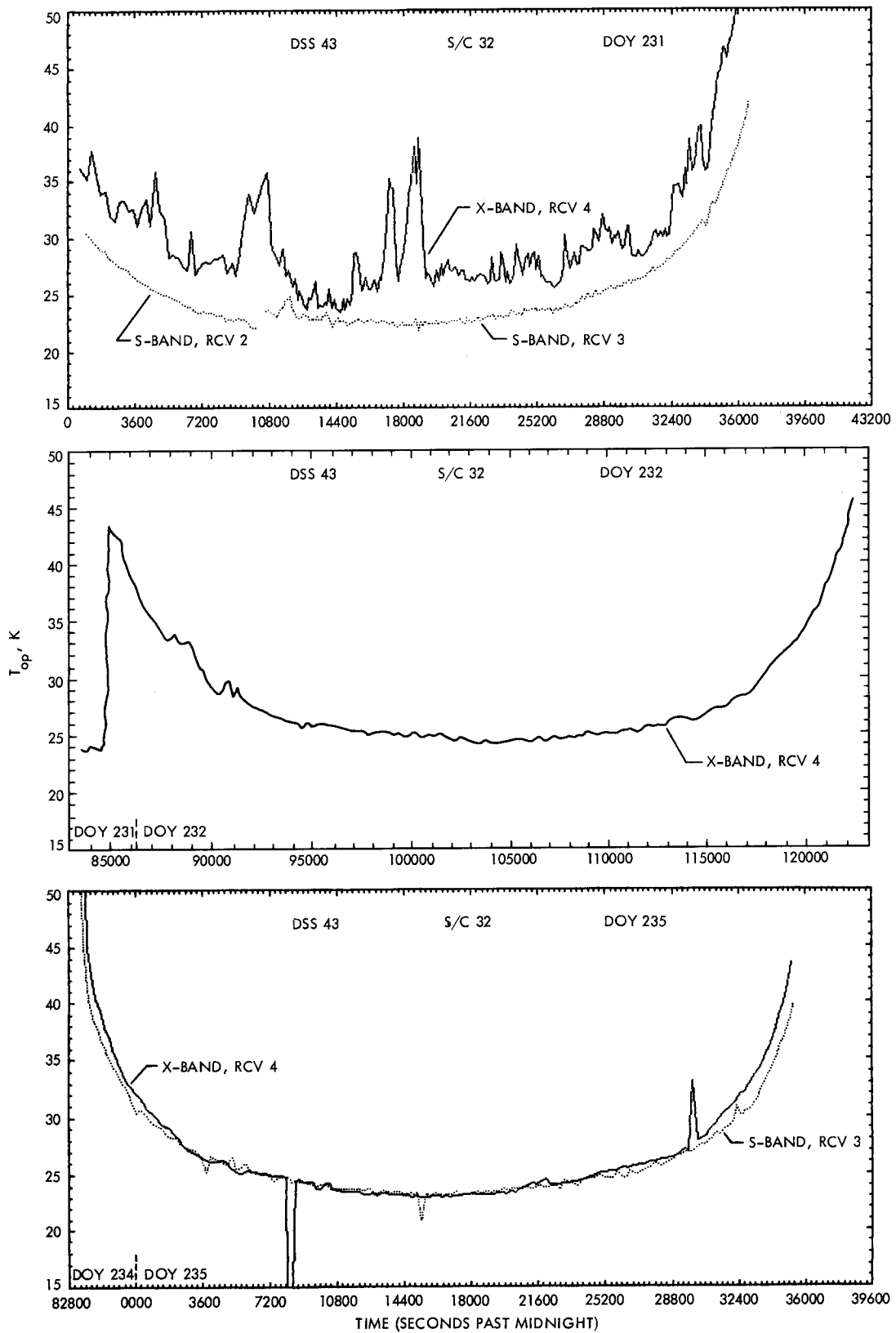


Fig. 11. System noise temperature plot—Australia

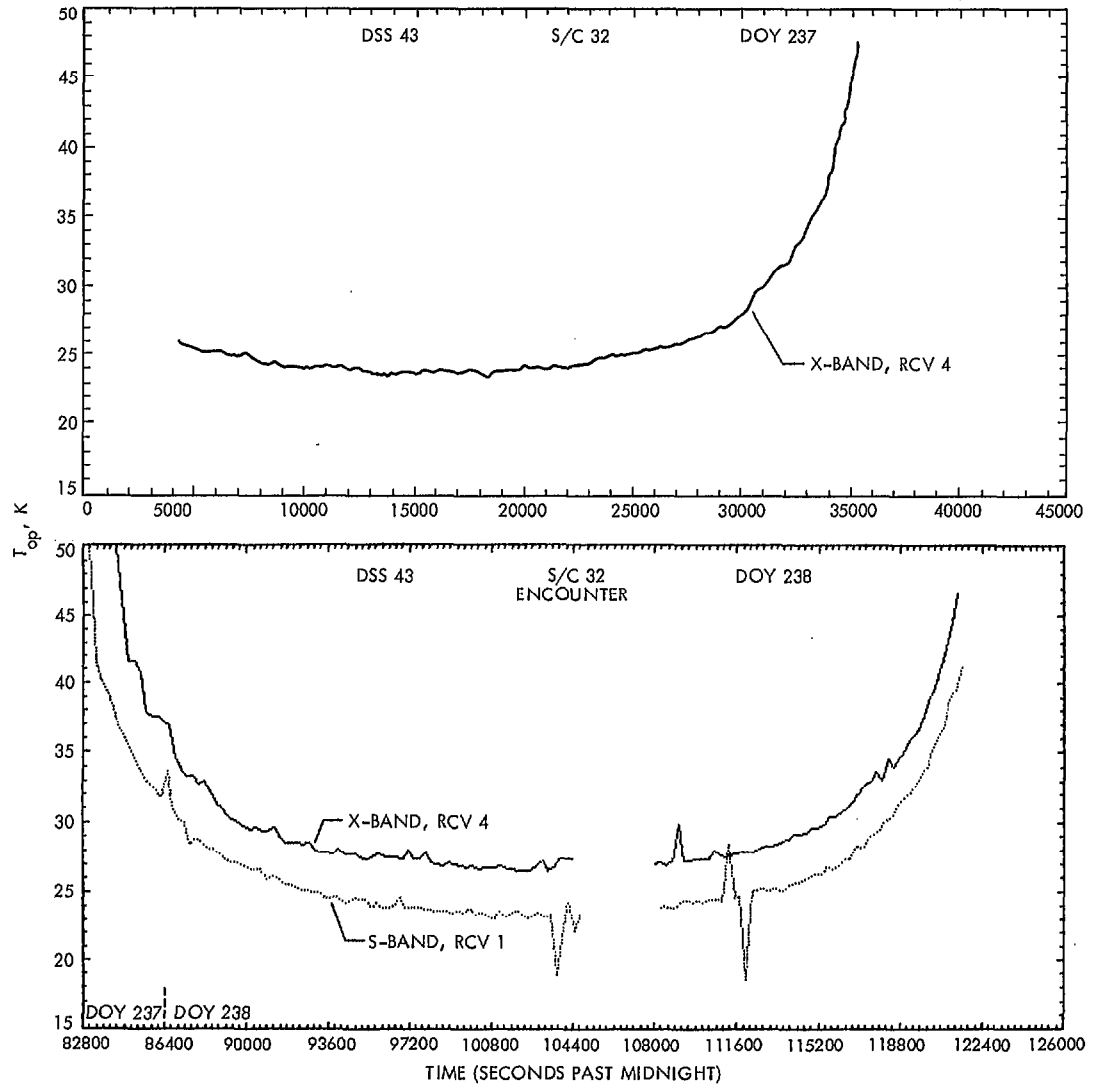


Fig. 11 (contd)

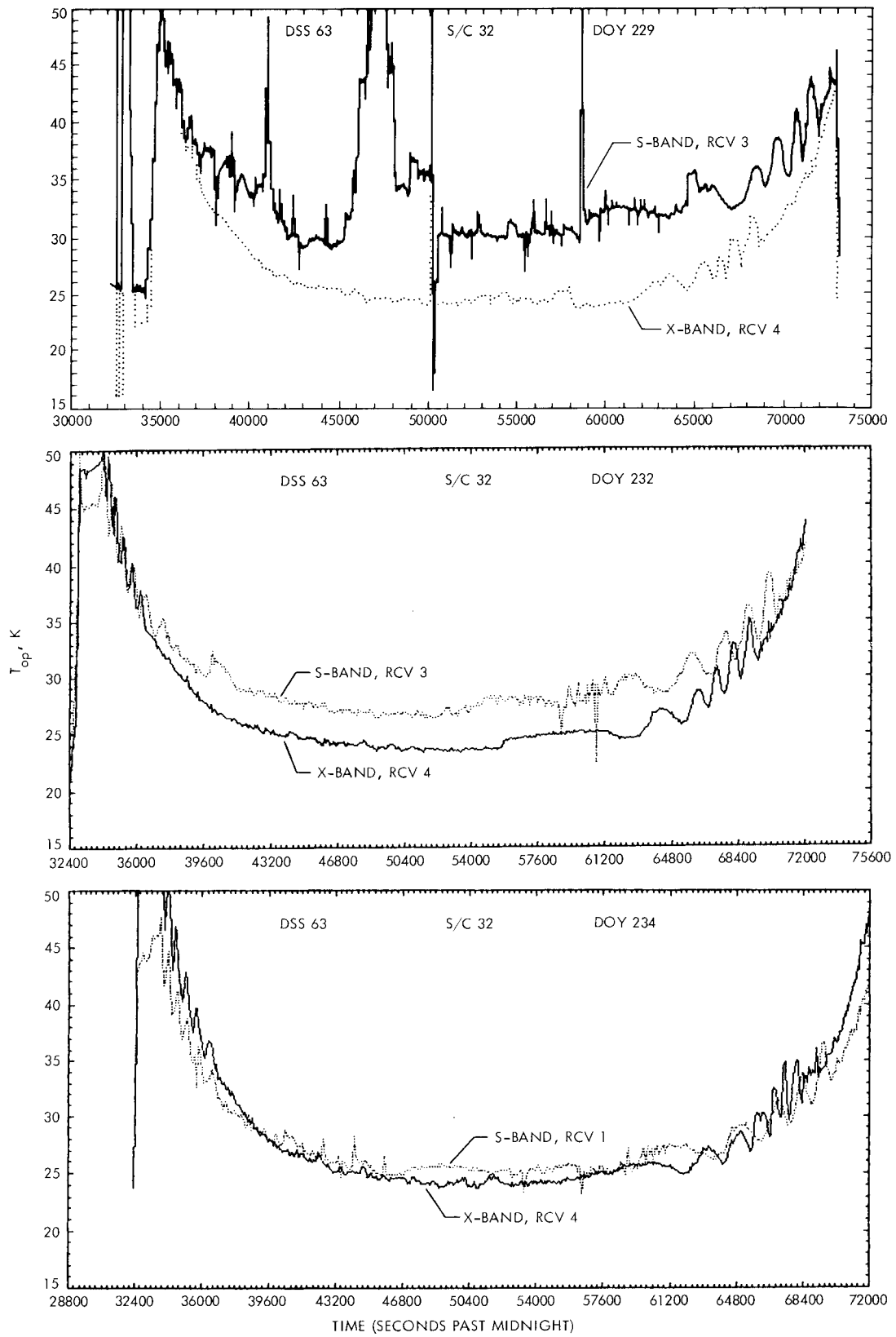


Fig. 12. System noise temperature plot—Spain

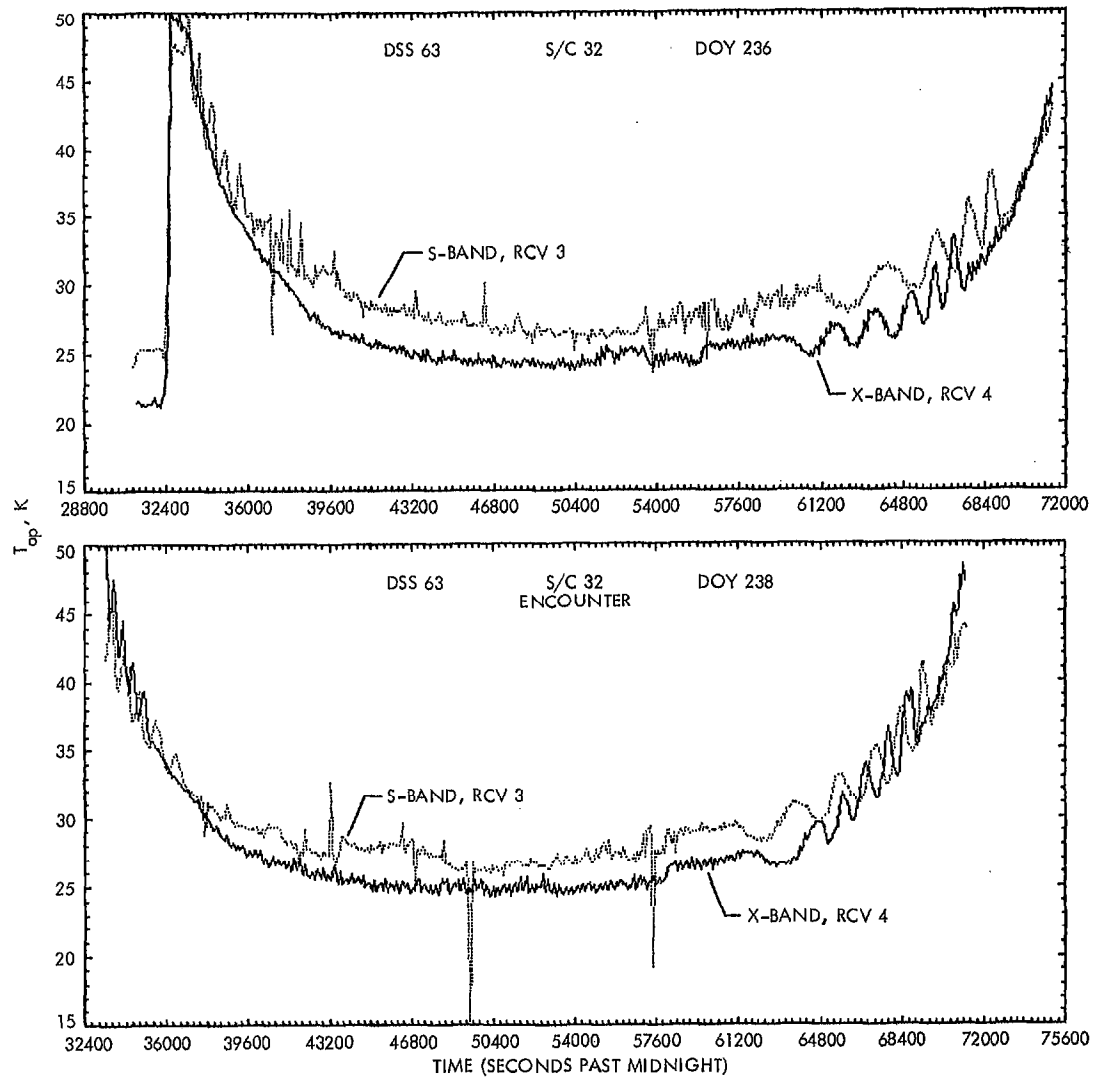


Fig. 12 (contd)